

1
2
3
4 **Extruded Polycarbonate/Di-Allyl Phthalate Composites with Ternary**
5
6 **Conductive Filler System for Bipolar Plates of Polymer Electrolyte Membrane**
7
8
9 **Fuel Cells**
10

11
12 *Ahmed Naji^a, Beate Krause^b, Petra Pötschke^b, Amir Ameli^{a*}*
13

14
15 *^aAdvanced Composites Laboratory, School of Mechanical and Materials Engineering,*
16

17 *Washington State University, 2710 Crimson Way, Richland, WA 99354, USA*
18

19
20 *^bDepartment of Functional Nanocomposites and Blends, Leibniz Institute of Polymer Research*
21

22 *Dresden, Hohe Straße 6, D-01069 Dresden, Germany*
23

24
25 ** Corresponding Author: Tel: 509-372-7442. Email: a.ameli@wsu.edu (Amir Ameli)*
26
27

28 **ABSTRACT**
29

30
31 Here, we report multifunctional polycarbonate (PC)-based conductive polymer composites
32 (CPCs) with outstanding performance manufactured by a simple extrusion process and intended
33 for use in bipolar plate (BPP) applications in polymer electrolyte membrane (PEM) fuel cells.
34 CPCs were developed using a ternary conductive filler system containing carbon nanotube (CNT),
35 carbon fiber (CF), and graphite (G) and by introducing di-allyl phthalate (DAP) as a plasticizer to
36 PC matrix. The samples were fabricated using twin-screw extrusion followed by compression
37 molding and the microstructure, electrical conductivity, thermal conductivity, and mechanical
38 properties were investigated. The results showed a good distribution and dispersion of the fillers
39 with some degree of interconnection between dissimilar fillers. The addition of DAP enhanced the
40 electrical conductivity and tensile strength of the CPCs. Due to its plasticizing effect, DAP reduced
41 the processing temperature by 75°C and facilitated the extrusion of CPCs with filler loads as high
42
43
44
45
46
47
48
49
50
51
52
53
54
55
56
57
58
59
60

1
2
3 as 63wt.% (3wt.% CNT, 30wt.% CF, 30wt.% G). Consequently, CPCs with the through-plane
4 electrical, in-plane electrical and thermal conductivities and tensile strength of $4.2\text{S}\cdot\text{cm}^{-1}$,
5 $34.3\text{S}\cdot\text{cm}^{-1}$, $2.9\text{W}\cdot\text{m}^{-1}\cdot\text{K}^{-1}$, and 75.4MPa , respectively, were achieved. This combination of
6 properties indicates the potential of PC-based composites enriched with hybrid fillers and
7 plasticizer as an alternative material for bipolar plate application.
8
9

10
11
12 **KEYWORDS:** Conductive polymer composites, bipolar plates, fuel cell, hybrid fillers, extrusion,
13 electrical and thermal conductivity, mechanical properties
14

15 16 17 18 19 20 21 22 23 24 25 26 27 28 29 30 31 32 33 34 35 36 37 38 39 40 41 42 43 44 45 46 47 48 49 50 51 52 53 54 55 56 57 58 59 60

Nowadays, green and sustainable energy sources represent one of the most attractive topics in the energy sector. Fuel cells are one of the electrical power sources that attract significant attention, due to their long life and less maintenance expenses. One of the most promising fuel cell types in portal and stationary applications is the polymer electrolyte membrane fuel cell (PEMFC). Bipolar plates (BPP) represent one of the main components of the PEMFCs, accounting for up to ~ 80% and 30-40% of total weight and cost, respectively, of a PEMFC fuel cell [1]. Graphite BPP is currently used in commercial PEMFCs because of its high electrical conductivity and good corrosion resistivity [2]. However, graphite brittleness results in poor mechanical properties and high machining costs of the flow channels [3]. These drawbacks of the graphite BPP drives the motivation to search for alternative materials [4, 5].

The biggest challenge for BPP designers is how to reduce the cost/weight while achieving a certain level of electrical, thermal, and mechanical properties. Metallic plates are an alternative proposed to replace graphite BPPs. Metallic BPPs offer excellent electrical and thermal conductivities [3, 6] with good mechanical properties [7]. However, the poor corrosion resistance of metals is the main drawback of metallic plates. Some technologies have been applied to

1
2
3 minimize the corrosion, such as using a paint of noble metal or aluminum electroplating [8, 9].
4
5 However, these paints increase the cost and the thickness. Using a thin layer of polymer as a binder
6
7 is another proposed way to reduce the corrosion of metallic BPPs [10]; these layers however
8
9 increase the cost and surface resistance.
10
11

12
13 Recently, researchers have prepared bipolar plates based on conductive polymer composites
14
15 (CPCs) to overcome the aforementioned disadvantages. Besides applications in bipolar plates [11,
16
17 12, 13, 14], CPCs have recently been investigated for many other applications, such as
18
19 electromagnetic interference shielding [15, 16, 17] and charge storage [18, 19, 20]. The reason for
20
21 this is that CPCs offer unique characteristics with tunable electrical and thermal conductivity, good
22
23 corrosion resistance, and high specific mechanical properties, as well as low weight and low cost.
24
25
26

27
28 In the production of BPPs, several CPCs with carbon-based fillers have been investigated [2,
29
30 21, 22]. Compared to graphite BPPs, CPC-based BPPs can exhibit better mechanical properties at
31
32 lower densities. They also have higher corrosion resistance, compared to metallic plates. As
33
34 thermoplastic polymers offer recyclability, they have been used numerously in preparing CPCs for
35
36 BPPs. Examples include polypropylene (PP) [14, 23, 24, 25], polyethylene (PE) [26], and
37
38 polyphenylene sulfide (PPS) [27, 28], filled with carbon fiber (CF) [12], Graphite (G) [11, 29],
39
40 carbon nanotube (CNT) [30, 31], carbon black (CB) [32, 33], and graphene (Gr) [12, 34], or
41
42 combinations of these fillers [35].
43
44
45

46
47 In general, conductivity increases with increasing filler content, but mechanical strength
48
49 decreases. A CPC-based BPP should be designed to have a balance between these two competing
50
51 characteristics. Through-plane and in-plane electrical conductivities of 1.1 and 1.9 S.cm⁻¹,
52
53 respectively, were reported for PE filled with 63wt.% G [36]. Filler loadings as high as 80wt.%
54
55 [37, 38] and 90wt.% [23] have been used to increase the conductivity; this is however at the
56
57
58
59
60

1
2
3 expense of the mechanical properties. Adding a modifier such as impact modifier can improve the
4 mechanical properties [39]. For instance, Hopmann et al. [23] reported a 99% increase in the
5 mechanical properties [39]. For instance, Hopmann et al. [23] reported a 99% increase in the
6 impact strength of PP-60wt.% graphite composite by introducing 30wt.% EPDM rubber relative
7 to PP mass, accompanied with only a small range decrease in conductivity. Another strategy for
8 the enhancement of electrical, thermal, or mechanical properties in nanocomposites is the surface
9 treatment of the nanofillers or the addition of a third component compatible with both nanomaterial
10 and the matrix [40, 41, 42].
11
12
13
14
15
16
17
18

19
20 The use of hybrid filler systems represents another effective strategy to enhance the
21 conductivity or lower the filler loading in CPCs. Kiraly and Ronkay [43] prepared nanocomposites
22 of PP filled with CB and G and assessed their applicability as BPP. They found that adding G as
23 the secondary filler enhanced the electrical conductivity and the flexural modulus but decreased
24 the tensile and impact strengths. Krause and Pötschke [44] prepared PP composite filled with
25 ternary filler system consisting of CNT, CF and GNP with total loading of 2.5vol.% of each filler.
26 They found that a proper selection of the filler system increases the thermal conductivity from 0.26
27 to 0.45 W.m⁻¹.K⁻¹ and the electrical conductivity from 10⁻¹⁷ to 10⁻³ S.cm⁻¹. Adloo et al. [14] used
28 PP filled with G, Gr, and nano-carbon black (NCB) together with maleic anhydride grafted PP as
29 a compatibilizer to prepare CPC for BPP and reported a through-plane electrical conductivity of
30 11.4 S.cm⁻¹ at 72wt.% total loading.
31
32
33
34
35
36
37
38
39
40
41
42
43
44

45
46 Johnson [45] used PP filled with ternary filler system of 2.5wt.%CB, 65wt.%G and 6wt.%CNT
47 to manufacture BPP and reported the in-plane electrical, in-plane thermal, and through-plane
48 thermal conductivities as 91 S.cm⁻¹, 24 W.m⁻¹.K⁻¹, and 6.55 W.m⁻¹.K⁻¹, respectively, but no
49 mechanical property data were reported. In another work, Yeetsorn [46] prepared a CPC of PP
50 filled with G, CB, chopped carbon fiber (CCF) and milled carbon fiber (MCF). They used a total
51
52
53
54
55
56
57
58
59
60

1
2
3 filler loading of 55wt.% and reported through-plane, in-plane electrical conductivity and thermal
4 conductivity values of $\sim 1.2 \text{ S.cm}^{-1}$, 13.0 S.cm^{-1} , $0.31 \text{ W.m}^{-1}.\text{K}^{-1}$. However, they failed to obtain
5
6
7 tensile strength results because of the composite brittleness. Recently, Naji et al. reported a PC-
8
9
10 based composite filled with CNT, CF, and G prepared through solution casting and systematically
11
12 studied the effects of filler contents at a constant total filler content (63wt.%) and found that the
13
14 highest conductivity is obtained when CNT and CF loadings are slightly above their percolation
15
16 thresholds [35].
17

18
19
20 Overall, a high filler loading ($>50\text{wt.}\%$) is needed to achieve an acceptable level of
21
22 electrical and thermal conductivities suitable for BPP application. In contrast to solution casting
23
24 [35] and thermosetting matrix cases, where filler wetting is achievable at filler loadings of up to
25
26 90wt.%, the high melt viscosity during thermoplastic processing represents a challenge for filler
27
28 wetting and composite extrusion process for CPCs with high filler content. It is therefore necessary
29
30 to solve this problem by reducing the CPC viscosity or increasing the wettability of the filler. To
31
32 achieve these effects, the present paper proposes the use of a plasticizer as a strategy and
33
34 investigates the effect of the selected di-allyl phthalate (DAP) on the properties of CPCs.
35
36
37

38
39 Therefore, CPCs based on polycarbonate (PC) were prepared by laboratory scale melt
40
41 compounding and compression molding to manufacture materials to be used in bipolar plates. The
42
43 compositions of the CPCs filled with hybrid fillers of CNT, CF, and G were selected based on an
44
45 earlier study [35]. The effects of CNT as a single filler in PC and as a secondary filler in PC-CF
46
47 were first investigated. Then, a ternary filler system of CNT, CF and G was applied. As the PC has
48
49 a high melt viscosity, there were difficulties in the extrusion of PC with high loading of fillers. For
50
51 the CPC with a filler combination of 3wt.%CNT, 20wt.%CF and 30wt.%G, a reduction of the melt
52
53 viscosity of the composite was achieved when DAP was used as plasticizer. The microstructure,
54
55
56
57

1
2
3 through-plane and in-plane electrical conductivity, as well as thermal conductivity and mechanical
4
5 properties were investigated to explore the plasticizer's effect.
6
7

8 **2. EXPERIMENTAL PROCEDURE**

9

10 **2.1. Materials**

11
12
13
14 Lexan grade ML9103 from SABIC Company was used as the polycarbonate (PC) matrix.
15
16 Carbon fiber (CF), grade of Px35CA0250-65 was supplied by Zoltek Corporation (St. Louis, MO,
17
18 USA), graphite (G), grade of 4439FM was provided by Asbury Carbons Inc. (Asbury, NJ USA),
19
20 multiwalled carbon nanotube (CNT), grade of Nanocyl[®] NC7000[™] was purchased from Nanocyl
21
22 S.A. (Sambreville, Belgium), and di-allyl phthalate (DAP), grade of ACROS 98% AC27662-2500
23
24 was provided by VWR Company (Radnor, PA, USA). CNT was provided with 90% purity having
25
26 an average diameter of 9.5nm and an average length of 1.3 μ m [47, 48].
27
28
29

30
31 The CNT and PC were dried and compounded using a twin-screw extruder to produce a
32
33 masterbatch of PC-10wt.%CNT. The compounding process was done using a Krauss Maffei
34
35 Berstorff ZE 25, with a screw length-to-diameter (L/D) ratio of 36, a screw rotational speed of
36
37 300rpm, and a throughput 10kg/h. PC was fed in the main hopper and CNT was dosed into the
38
39 side feeder attached at 14D position of the screw length. This PC-10wt.%CNT masterbatch was
40
41 then used as the supply of CNT for all the samples reported in this work.
42
43
44

45 **2.2. Sample preparation**

46
47
48 Table 1 shows the design of experiment used to prepare CPCs. The compositions were selected
49
50 based on a previous solution casting study of similar formulation [35]. In Table 1, the symbols C,
51
52 N, F, G, D denote polycarbonate, carbon nanotube, carbon fiber, graphite and DAP, respectively.
53
54 The numbers next to these letters represent the weight percentage of the corresponding component,
55
56
57
58
59
60

e.g., CN3F20G30D30 means PC with 3wt.%CNT, 20wt.%CF, and 30wt.%G with a DAP amount of 30wt.% relative to the PC weight (10.8wt.% relative to the total weight of the composite).

Table 1: Design of experiment for testing various compositions of the PC-based CPCs.

Code	Compositions (wt.%)				
	PC	CNT	CF	G	DAP
CN1	99	1	-	-	-
CN3	97	3	-	-	-
CN5	95	5	-	-	-
CN3F10	87	3	10	-	-
CN3F20	77	3	20	-	-
CN3F20	67	3	30	-	-
CN3F10G30	57	3	10	30	-
CN3F20G30	47	3	20	30	-
CN3F20G30D30	36.2	3	20	30	10.8
CN3F30G30D30	28.5	3	30	30	8.5

All the materials except DAP were dried at 100°C and -80kPa of vacuum for 4h to remove any moisture. Different weight percentages of masterbatch, fillers (CF and G), pure PC, and DAP were then dry mixed and fed into the hopper and extruded. The extrusion process was conducted using a 16mm twin-screw extruder with an L/D ratio of 40 (type LTE, LabTech Engineering Company LTD., Muang, Samutprakarn, Thailand) at a fixed screw speed of 20rpm and different temperature profiles (measured by the thermocouples mount on the extruder barrel) for each composition, as will be discussed in section 5.2.3. The extruded filaments were then pelletized and compression molded using a hydraulic hot press (Model: 3851-0, SN:150130 CARVER INC., USA) in a temperature range of 250-300°C and time range of 10-20min to prepare the samples for conductivity and tensile test measurements. The conductivity samples had dimensions of 1.5×15×40mm³ and the tensile samples were made according to ASTM D3039 Type IV.

3. CHARACTERIZATION

3.1. Microstructure and morphology

To investigate the microstructure of the prepared nanocomposites in term of the filler's morphology and their dispersion and distribution within the matrix, scanning electron microscopy (SEM) was conducted. CN3F30G30D30 sample was examined as it offered the best overall performance. The compression-molded samples were cryofractured, sputter coated with 3nm platinum, and imaged using an SEM Zeiss UltraPlus at an acceleration voltage of 3kV by applying the SE2 detector.

3.2. Through-plane electrical conductivity

As shown in Figure 1a, a simple device was built to test the through-plane electrical conductivity according to the requirements given by the US Fuel Cell Council [49]. It is made of two smooth-surfaced copper plates as the probes, connected to a voltmeter (V) and an ammeter (A). In this test, the sample was placed between the two probes and compressed using a hydraulic press [49]. V and I were measured six times per minute per sample and the resistance was calculated using:

$$R_{sample} = \frac{1}{N} \times \sum_{n=1}^{n=N} R_n - R_{tools} \quad (1)$$

where R_{sample} , R_n , R_{tools} and N are the Ohmic resistance of the sample, total resistance of the probes with the sample, the resistance of the probes without sample, and the number of readings per sample, respectively. The resistivity was then obtained as:

$$\rho_{sample} = \frac{W \times L \times R_{sample}}{T} \quad (2)$$

where T , W , L are the sample's thickness, width, and length, respectively. Lee et al. [50, 51] used the area specific resistance (ASR) as another conductivity characteristic with a maximum desirable value of $0.03 \Omega \cdot \text{cm}^2$ for BPP application. ASR is defined as the resistance through the thickness and tested using the same through-plane conductivity apparatus (Figure 1a) and calculated using the following equation:

$$ASR = (R_n - R_{tools}) \times W \times L \quad (3).$$

3.3. In-plane electrical conductivity

For in-plane conductivity measurements, an additional device according to ASTM D4496 [52, 53] was built. In this setup, four lined copper metal rods were used as probes, as show in Figure 1b. The two outer probes carry a DC current (I), supplied by a DC power supplier, while the two inner probes measure the voltage (V). The sample resistivity was then obtained using [54]:

$$\rho_{sample} = \frac{W \times T \times R_{sample}}{L_p} \quad (4)$$

where L_p is the distance between the inner probes. The electrical conductivity, σ was then calculated as the reciprocal of ρ_{sample} .

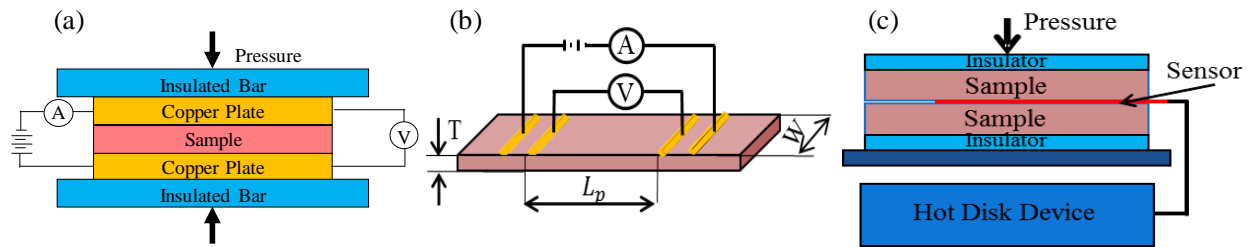


Figure 1: Schematic representations of the characterization devices used for the measurement of (a) through-plane electrical conductivity, (b) in-plane electrical conductivity, and (c) thermal conductivity.

3.4. Thermal conductivity

1
2
3 A hot disk analyzer, TPS 500S, ThermTest Inc. S/N 20140500235, Sweden, together with the
4
5 C7577 sensor with a radius of 2.0mm was used to measure the thermal properties of the
6
7 composites, as schematically shown in Figure 1c. Two samples of the same material were
8
9 sandwiched together with the sensor in between. The test directly provides the thermal
10
11 conductivity coefficient (k) [55].
12
13
14

15 **3.5. Tensile test**

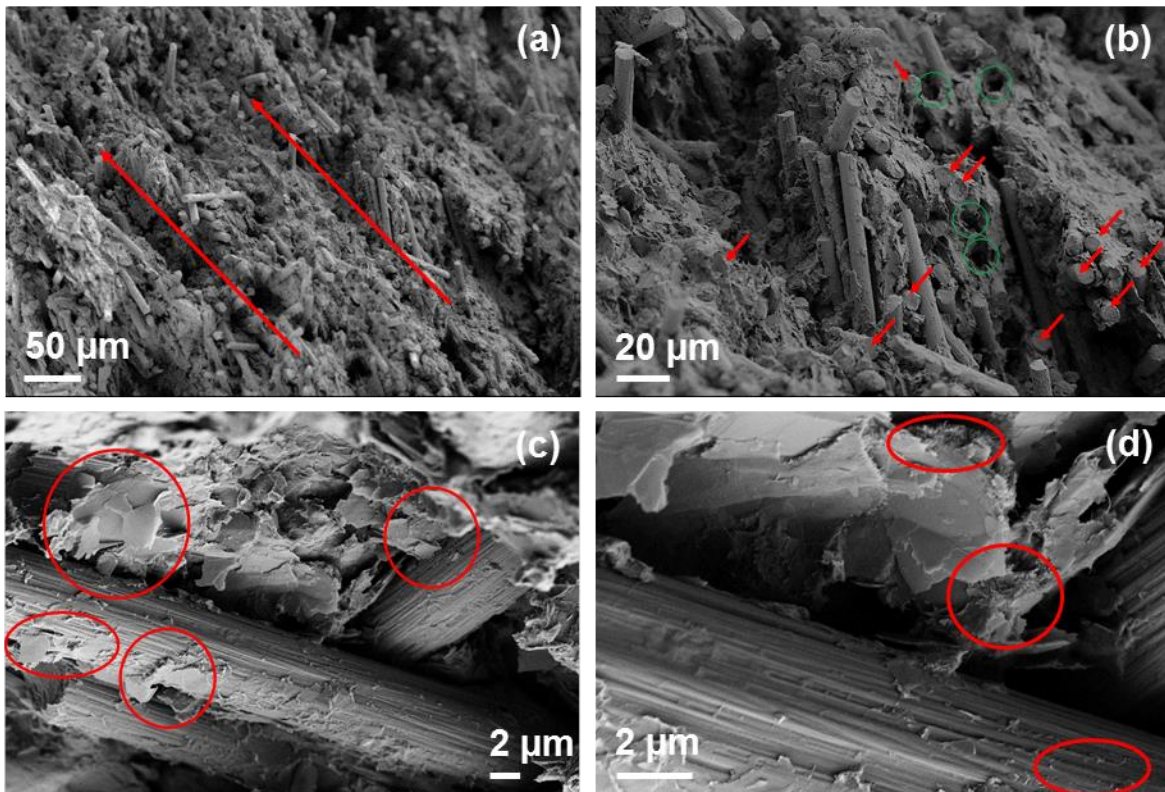
16
17
18 The tensile tests were conducted according to the ASTM D3039 standard with Type IV
19
20 specimen configuration using a custom load frame. For all the conductivity and tensile tests, at
21
22 least five samples were tested for each composite and their average values are reported here with
23
24 the error bars as the standard deviations.
25
26
27

28 **4. RESULTS AND DISCUSSION**

29 **4.1. Microstructure and morphology**

30
31
32
33 Since the composite morphology significantly affects the properties, it was first investigated
34
35 using SEM. Figure 2a-d shows cryofractured surfaces of the CN3F30G30D30 composite. CFs
36
37 showed a relatively uniform distribution with a slight preferred in-plane orientation, as shown by
38
39 the red arrows in Figure 2a. This alignment was caused by the compression molding process. As
40
41 the extruded pellets are randomly located in the compression mold, the alignment due to extrusion
42
43 process had less influence on the final CF orientation. Figure 2b provides an insight into the failure
44
45 mode of the composite. Most of CFs that were normal to the failure surface broke at the cross-
46
47 section of the failure surface without being pulled out, as denoted by red arrows in Figure 2b. This
48
49 is an indication of a good bonding between the fibers and the matrix as well as a sufficient fiber
50
51 length, which resulted in sufficient load transfer capability between the fibers and the matrix so
52
53
54
55
56
57
58
59
60

1
2
3 that their interface did not fail during cryofracturing. In Figure 2b, some pulled-out fibers are also
4
5 seen, which can be attributed to fibers with shorter length or fibers that were in contact with other
6
7 fillers, i.e., G and CNT. Figure 2c shows the G flakes with a size of several micrometers dispersed
8
9 in the polymer matrix, some of which are in physical contact with CFs. As seen in Figure 2d, also,
10
11 some CNTs were in contact with the surfaces of CF and G. While filler to filler contact is favorable
12
13 in enhancing the conductivities, it adversely affects the mechanical properties, as the load cannot
14
15 be effectively transferred between them.
16
17
18
19



46
47
48
49
50
51
52
53
54
55
56
57
58
59
60

Figure 2: SEM micrographs of the CN3F30G30D30 composite having 3wt.% CNT, 30wt.% CF, 30wt.% G, and 8.5wt.% DAP as plasticizer: (a) the overall microstructure showing the distribution and alignment of CFs; red arrows show the slight alignment of CFs, (b) CF breakage and pull-outs; red arrows and green circles point the CF breakage and pull-out, respectively, (c)

1
2
3 G flakes and their contact with CFs; red circles identify locations where G and CF contact
4
5 occurs, and (d) CNTs on the surfaces of G and CF; red circles mark the CNTs.
6
7

8 **4.2. Electrical conductivity**

9

10 *4.2.1. CPCs with single- and binary-filler systems*

11
12

13
14 High electrical conductivity is a prerequisite for the production of suitable BPP materials. The
15 through-plane and in-plane electrical conductivities of PC filled only with CNT are shown in
16 Figure 3. The conductivity values of PC-CNT composites suggests that the percolation threshold
17 is relatively low (<1.0wt.% CNT), which indicates a good dispersion of CNTs. The percolation
18 thresholds for twin-screw extruded and compression molded composite materials with the same
19 CNT type (but different PC type) was reported to be 0.25wt.% as measured in-plane [56]. Overall,
20 the in-plane conductivity is higher than the through-plane one, an effect that typically occurs with
21 fillers that tend to orient in-plane during shaping processes in sheet-like structures [57]. Therefore,
22 the conductive network is better developed in the in-plane direction. The in-plane conductivity
23 also showed a lower sensitivity to the CNT content than the through-plane conductivity. With the
24 increase of CNT content from 1 to 10wt.%, the in-plane conductivity increased by about one order
25 of magnitude, while the through-plane conductivity increased by two orders.
26
27
28
29
30
31
32
33
34
35
36
37
38
39
40
41
42
43
44
45
46
47
48
49
50
51
52
53
54
55
56
57
58
59
60

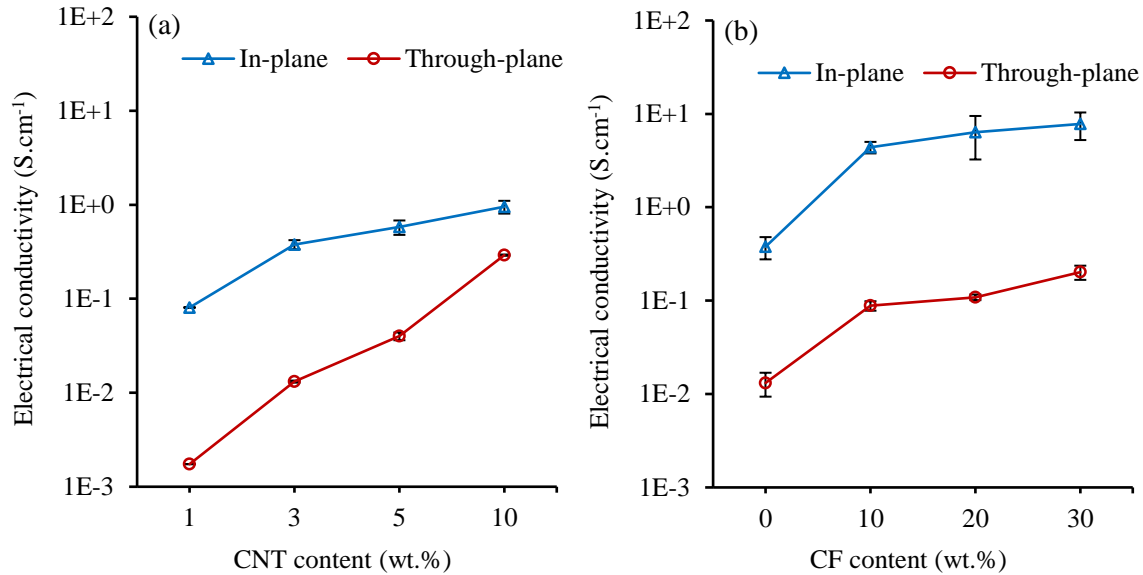


Figure 3: The variation of in-plane and through-plane electrical conductivities with (a) CNT content in the PC-based CPCs with single filler of CNT (PC-CNT) and (b) CF content in the CPCs with two fillers of CNT and CF (PC-3wt.%CNT-CF).

The use of CNT as a secondary filler can improve the electrical conductivity of CF filled polymers. This is due to the very high aspect ratio, the expected good dispersion, and the low percolation threshold of CNT. In addition, the two fillers with different length scales can promote conductivity by forming double-percolation networks and bridging between the fillers, which strengthens electron tunneling [49]. When designing binary and ternary filler systems, care must be taken to ensure that the CNT loading is well above the percolation threshold to make a positive contribution to improved conductivity and at the same time minimize the proportion of cost-intensive CNT. For this reason, 3wt.% was selected as the optimum CNT loading for the hybrid composites.

Figure 3b shows the effect of CF content on the through-plane and in-plane conductivities of PC-3wt.%CNT-CF composites. The introduction of 10wt.%CF in PC-3wt.%CNT resulted in an

1
2
3 increase in conductivity of about one order of magnitude both in-plane and through-plane. When
4
5 the CF content was increased from 10 to 30wt.%, the conductivity increased only slightly,
6
7 indicating that PC-3wt.%CNT-10wt.%CF already had a well percolated network. It is also noted
8
9 that the introduction and variation of CF content did not affect the conductivity anisotropy of the
10
11 composites. The highest through-plane and in-plane conductivities in composites with binary
12
13 fillers were $0.2\text{S}\cdot\text{cm}^{-1}$ and $7.8\text{S}\cdot\text{cm}^{-1}$, respectively, for PC-3wt.%CNT-30wt.%CF. These value are
14
15 still not high enough for BPP applications based on the US Department of Energy (DOE) targets,
16
17 which will be discussed later in Table 2. Therefore, G was chosen as a third filler to further improve
18
19 the electrical conductivities.
20
21
22
23
24
25

26 *4.2.2. CPCs with ternary filler system*

27
28
29

30 In the CPCs with a ternary filler system, the overall filler loading was up to 63wt.%; CNT and
31
32 G loadings were maintained unchanged at 3wt.% and 30wt.%, respectively [35], while CF content
33
34 was varied at 10, 20, and 30wt.%. The composite CN3F10G30 had a total filler loading of 43wt.%
35
36 and could be extruded without processing problems. When the CF content was increased to
37
38 20wt.% (CN3F20G30 composite with a total filler loading of 53wt.%), extrusion difficulties
39
40 occurred and extrusion processing became impossible for composites with filler loadings greater
41
42 than 53wt.%. It is known that increasing filler content within a polymer matrix increases the overall
43
44 viscosity and that an increase in the processing temperature of the composite material can be used
45
46 to counteract this, provided that the respective polymer matrix permits this without excessive
47
48 degradation. However, this is not possible in all cases and too high composite viscosity makes the
49
50 extrusion process challenging or sometimes impossible. In order to mitigate this problem and
51
52 facilitate the fabrication of composites with higher filler loadings, it was decided to use a plasticizer
53
54
55
56
57
58
59
60

that can effectively decrease the melt viscosity. It is reported that the use of di-allyl phthalate (DAP) by 40wt.% relative to PC weight can reduce the PC's melting temperature from 250 to 180°C [58]. Moreover, due to the enhanced wetting of the fillers in the presence of a plasticizer, it was expected that DAP could also improve some of the physical and mechanical properties. Therefore, a DAP content of 30wt.% relative to PC weight (Table 1) was added to the CN3F20G30 and CN3F30G30 composites to enable the reduction of the processing temperatures due to the reduced melt viscosity. As seen in Figure 4, increasing the CF content from 10 to 20wt.% required a general increase in the temperature profile in order to extrude the material, where the maximum temperature reached 310°C; this was the maximum allowable temperature for PC processing. However, adding DAP to the CN3F20G30 composite enabled the reduction of the maximum temperature by 70°C from 310°C to 240°C. Hence, the extrusion of composites with filler loading more than 53wt.% became possible and CN3F30G30 with 63wt.% total filler loading was also successfully extruded with a maximum temperature of 285°C.

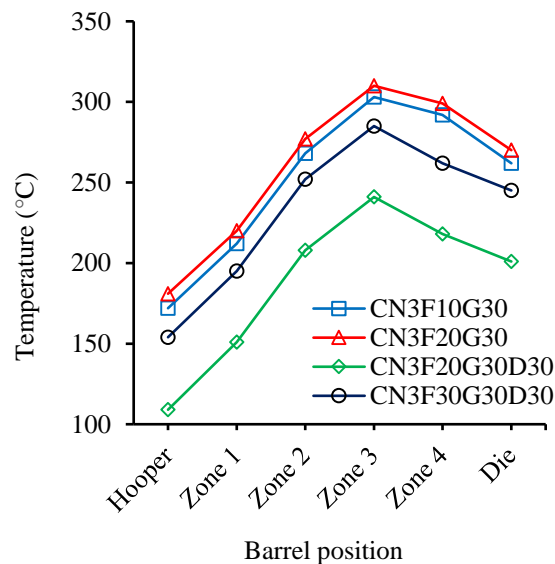
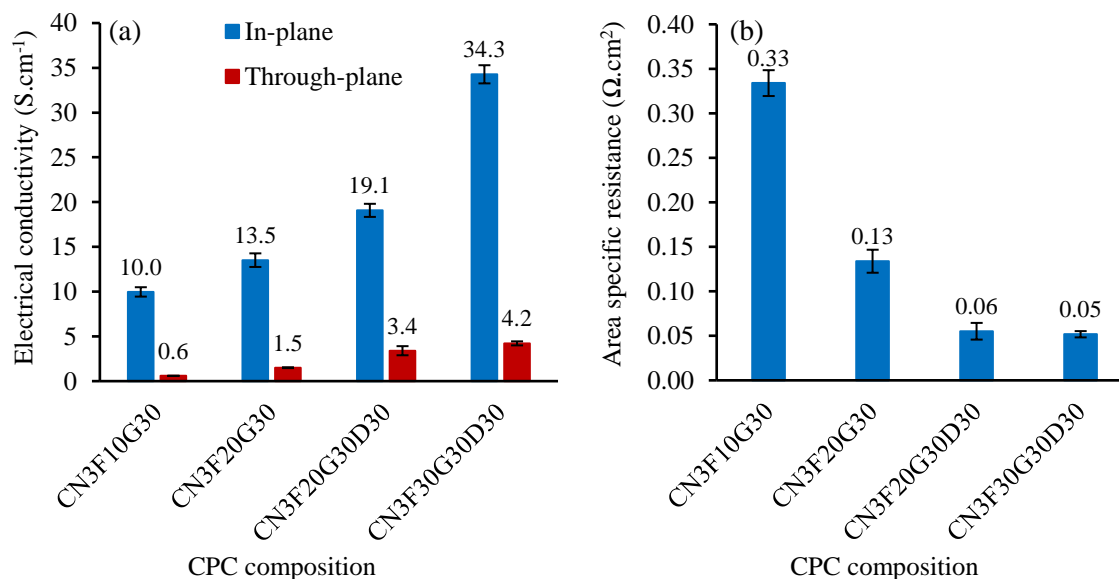


Figure 4: Extrusion temperature profiles used in the fabrication of PC-based CPCs filled with ternary filler system, without and with DAP as plasticizer.

Figure 5a shows the through-plane and in-plane conductivities of the ternary CPCs with and without DAP as plasticizer. Introducing 30wt.%G to PC-3wt.%CNT-10wt.%CF increased the through-plane and in-plane conductivities by 6.7 and 2.3 times, reaching values of 0.6 and 10.0S.cm⁻¹, respectively. Once the CF content was increased from 10 to 20wt.% (CN3F20G30 sample), the through-plane and in-plane conductivities further increased to 1.5 and 13.5S.cm⁻¹, respectively. With the introduction of DAP to the CN3F20G30 composite (with 53wt.% total filler), the through-plane and in-plane electrical conductivities were raised to 3.4 and 19.1S.cm⁻¹, accounting for 120% and 40% enhancement, respectively. In the presence of DAP, the CF content could be raised to 30wt.% in CN3F30G30 sample (63wt.% total filler load), which resulted in further increase of the conductivity to 4.2 and 34.3S.cm⁻¹ in the through-plane and in-plane directions, respectively. Achieving this level of conductivity is a step closer to the US DOE target of 20 and 100S.cm⁻¹ for the through-plane and in-plane conductivities [59]. More discussion and comparison with the current literature will be given in section 4.5.



1
2
3 Figure 5: The variation of (a) in-plane and through-plane electrical conductivities and (b) area
4 specific resistance (ASR) at different compositions of PC-based CPCs filled with CNT, CF, and
5 G, without and with DAP as plasticizer.
6
7
8
9
10

11 Moreover, as shown in Figure 5b, the ASR of the ternary composites decreased with increasing
12 CF content and the introduction of DAP. Increasing the CF content from 10 to 20wt.% reduced
13 the ASR from 0.33 to 0.13 Ω .cm² and subsequently adding DAP to the CN3F20G30 composite
14 further reduced the ASR from 0.13 to 0.6 Ω .cm², representing a resistance reduction of more than
15 50%. The CN3F30G30D30 showed an ASR of 0.05 Ω .cm², which is close to the recommended US
16 DOE target of 0.03 Ω .cm². In summary, the addition of DAP as a plasticizer lowered the viscosity
17 of overall composite during extrusion and improved wetting and mixing of the fillers, resulting in
18 improved electrical properties.
19
20
21
22
23
24
25
26
27
28
29
30
31

32 **4.3. Thermal conductivity**

33 *4.3.1. CPCs with single- and binary-filler systems*

34
35 The BPP's thermal conductivity is very important for the heat transfer between the components
36 of a PEMFC. Results for the composites filled with CNT as single filler are shown in Figure 6a.
37 The thermal conductivity increased only slightly as the CNT content was increases from 1 to
38 10wt.% and the highest conductivity of 0.59W.m⁻¹.K⁻¹ was obtained for PC-10wt.%CNT. For PC-
39 3wt.%CNT composite, unlike the relatively high electrical conductivity, the thermal conductivity
40 was 0.31W.m⁻¹.K⁻¹, only slightly higher than that of the pure PC (0.23W.m⁻¹.K⁻¹).
41
42
43
44
45
46
47
48
49
50
51

52 As shown in Figure 6b, the thermal conductivity in the binary composites of PC-3wt.%CNT-
53 CF increased continuously with CF content and reached a value of 0.85W.m⁻¹.K⁻¹ at 30wt.%CF.
54
55
56
57
58
59
60

Overall, the thermal conductivity of the composites (Figure 6) was less affected by the CNT and CF content, compared to their electrical conductivity (Figure 3). Electrical and thermal conduction phenomena are governed by different mechanisms, namely electron transfer and phonon transfer, respectively. Electron transfer can be achieved through non-contact mechanisms such as electron tunneling and hopping. However, phonon transfer needs a good physical contact at the interfaces. Therefore, improving thermal conductivity is a greater challenge compared to electrical conductivity.

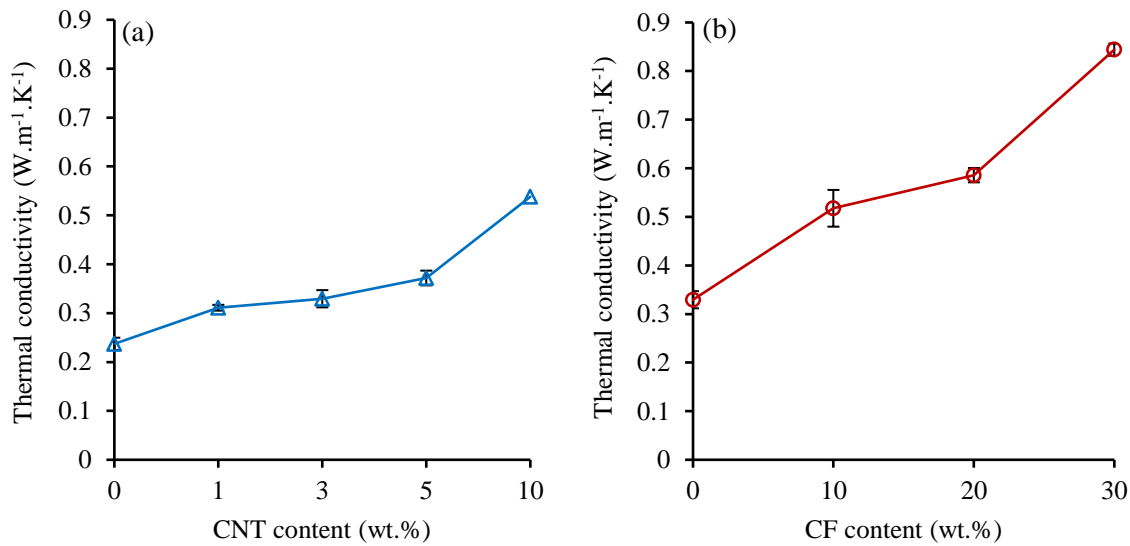


Figure 6: The variation of thermal conductivity with (a) CNT content in the PC-based CPCs with single filler of CNT (PC-CNT) and (b) CF content in the CPCs with two fillers of CNT and CF (PC-3wt.%CNT-CF).

5.3.2. CPCs with ternary-filler system

Figure 7 depicts the thermal conductivity of the ternary CPCs. Overall, an increase in the CF content and the introduction of DAP enhanced the thermal conductivity and a maximum thermal conductivity value of $2.9 \text{ W.m}^{-1}.\text{k}^{-1}$ was achieved for the CN3F30G30D30 composite with 63wt.%

total filler loading. As compared later in Table 2, this value exceeds the values given in the literature for the thermal conductivity of various composite materials (at similar filler loads) prepared for bipolar plate applications. A combination of several factors resulted in the enhanced thermal conductivity: a) multiple percolations at different length scales and/or interconnections between different filler types obtained by the use of G, CF, and CNT, b) a good dispersion and distribution of the fillers in the melt mixing process by significantly decreasing the viscosity through the addition of DAP as plasticizer, and c) relatively high loading of the conductive fillers. It is also noted that the highest electrical and thermal conductivities were obtained for the same composition i.e., CN3F30G30D30.

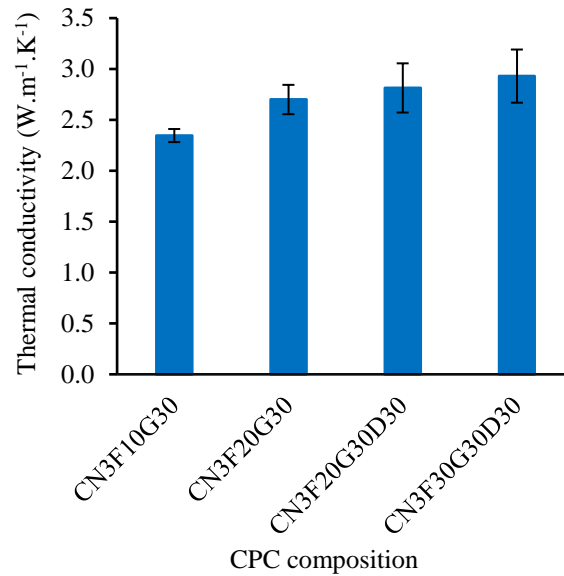


Figure 7: The variation of thermal conductivity with the composition in the PC-based CPCs filled with CNT, CF, and G without and with DAP as plasticizer.

4.4. Mechanical properties

4.4.1. CPCs with single- and binary-filler systems

1
2
3 In addition to the conductivity properties, BPP also requires a certain mechanical property
4 profile, which is mainly for the assembly process of the PEMFC. During this process, the BPP
5 should not break, which demands a certain strength and flexibility. As shown in Figure 8a, overall,
6 the tensile strength of PC-CNT decreased with the CNT content. The decrease is slight up to
7 3wt.%CNT, with values decreasing from 62.4 to 52.4MPa with the addition of 3wt.% CNT, but
8 further decreasing to 26.6MPa with 5wt.%CNT. Tensile strength reduction with the introduction
9 of CNT, even at low contents (0.1 and 0.5wt.%) is quite often found for PC matrices when no
10 compatibilizer is used [60, 61, 62]. This is due to the hindrance of the typical deformation
11 processes, which occurs in PC, when a nanostructured CNT network is overlaid. In addition, the
12 poor adhesion between CNT surface and PC molecules without a proper compatibilizer contributes
13 to that [63]. Since in this work no compatibilizer was used and the CNT content was also relatively
14 high (up to 5wt.%), the reduction in the strength is due to the combination of a highly percolated
15 fillers structure, poor interfacial adhesion, and the existence of remaining CNT agglomerates that
16 act as stress concentration locations and cause premature failure. As the CNT content increases,
17 complete dispersion becomes more difficult and thus the number and size of remaining
18 agglomerates increase, which further degrades the strength.

19
20
21
22
23
24
25
26
27
28
29
30
31
32
33
34
35
36
37
38
39
40
41 Figure 8b shows the effect of CF content on the tensile strength in the binary CPCs of PC-
42 3wt.%CNT-CF. The tensile strength continuously increased as the CF content was increased from
43 0 to 30wt.%. The addition of 30wt.%CF significantly increased the strength of binary CPCs from
44 52.4 to 124.9MPa. As CF is a micro-sized filler, it could be more easily distributed and dispersed
45 within the matrix (Figure 2a), and as discussed in section 5.1, a good bonding was formed between
46 CF and PC, which both contributed to the enhancement of the strength.

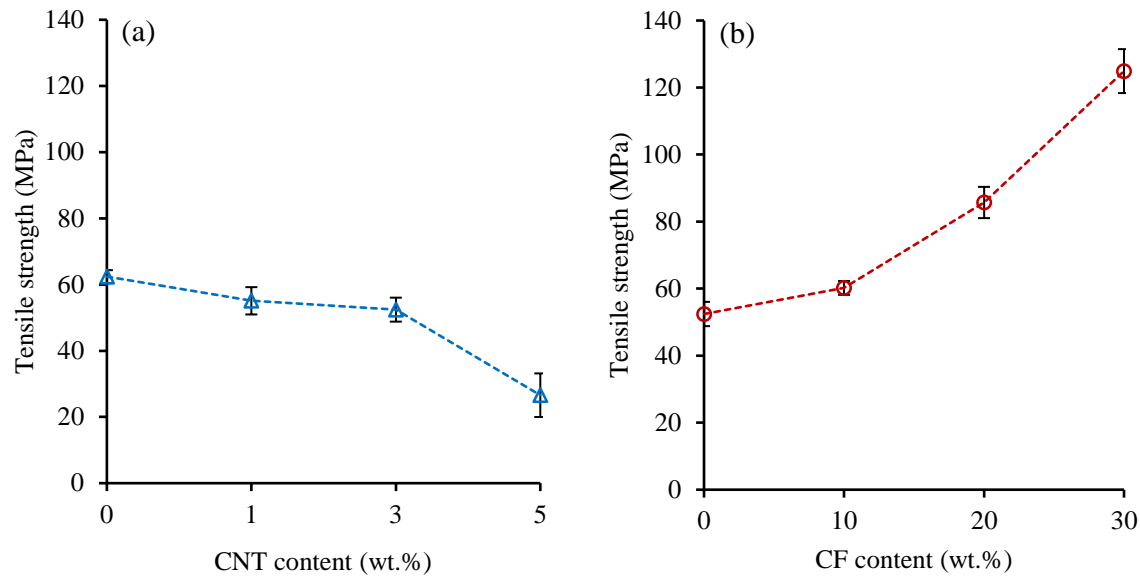


Figure 8: The variation of tensile strength with (a) CNT content in the PC-based CPCs with single filler of CNT (PC-CNT) and (b) CF content in the CPCs filled with two fillers of CNT and CF (PC-3wt.%CNT-CF).

4.4.2. CPCs with ternary-filler system

Figure 9a-b shows the tensile strength and Young's modulus of the ternary CPCs. At low CF content of 10wt.% CF, the addition of 30wt.% G (CN3F10G30 composite) enhanced the strength from 60.2 to 82.4MPa, indicating that at a total filler content of 43wt.%, both CF and G enhanced the strength. However, once 30wt.% G was added to the CPC with 20wt.% CF (CN3F20G30 composite), the strength decreased from 85.7 to 76.5MPa. Overall, at highly filled hybrid CPCs of thermoplastics prepared using melt mixing, there is a certain total filler loading beyond which the strength starts to decrease. This is because the dispersion and distribution of such a high amount of filler becomes difficult and the molten thermoplastic matrix cannot fully wet the fillers. Therefore, only a fraction of the fillers can make effective interfacial bonds with the matrix and

thus stress transfer efficiency decreases. Moreover, the chance of filler agglomeration increases as the filler load increases, which causes more local stress concentrations.

In the case of the CN3F20G30D30 composite, where DAP was added, the strength was slightly increased from 76.5 to 81.7MPa. While DAP, as a polymer with a much lower molecular weight compared to the PC matrix, decreases the overall strength of the matrix, its presence during the composite extrusion process reduced the melt viscosity, which could result in a better filler mixing and wetting and thus positively contributed to the strength of composite. The net effect of these two competing factors was a slight increase in the tensile strength. Once the CF content was further increased to 30wt.% (CN3F30G30D30), the strength dropped from 81.7 to 75.4MPa, due to the reasons discussed above. This value sufficiently exceeds the strength requirements of the US DOE and it is also higher than the values reported in the literature for other materials for BPP applications (see Table 2).

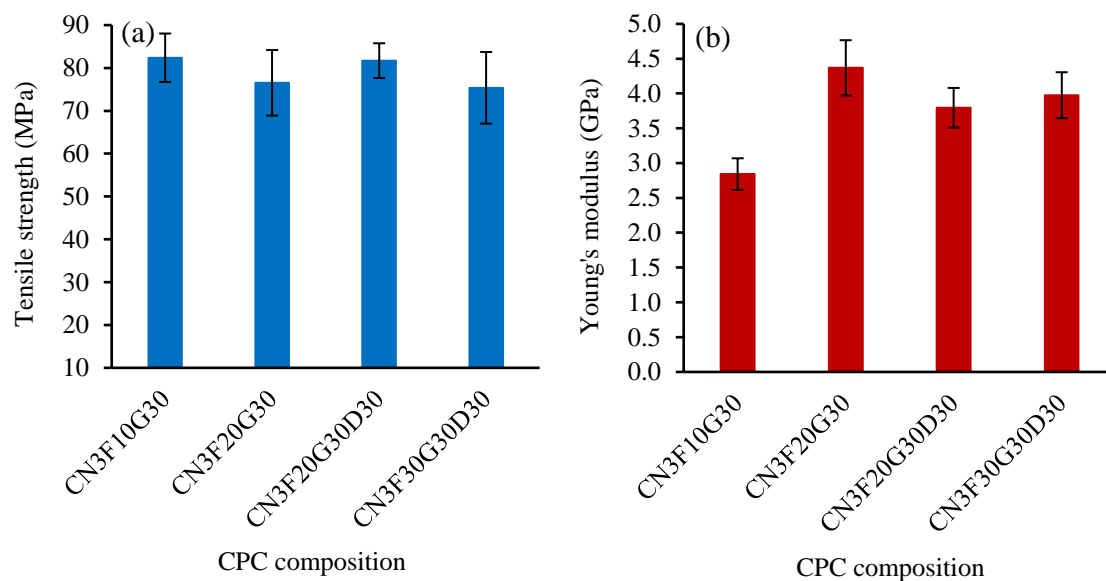


Figure 9: The variation of (a) tensile strength and (b) Young's modulus with composition in PC-based CPCs filled with CNT, CF, and G, without and with DAP as plasticizer.

1
2
3 An increase in the CF content resulted in an increase in the CPC's modulus of elasticity,
4 especially when the CF was increased from 10 to 20wt.%, the modulus was increased from 2.8 to
5 4.4GPa. On the other hand, the addition of DAP decreased the modulus to 3.8GPa in
6 CN3F20G30D30 composite. This was expected as the presence of DAP plasticizer makes the
7 slippage between the PC chains easier and thus the composite deforms at lower levels of stress,
8 resulting in a reduced stiffness. Finally, increasing the CF content to 30wt.% in the presence of
9 DAP (CN3F30G30D30 composite) raised the modulus slightly to 4.0MPa. Again, as the filler
10 content increases, full wrapping of the fillers with the matrix polymer chains becomes more
11 difficult and some unwrapped filler may slip over one another, and consequently, the modulus
12 does not further increase significantly.
13
14
15
16
17
18
19
20
21
22
23
24
25

26 ***4.5. Comparison of values with literature and requirements***

27
28
29 In order to compare the obtained results with the literature and the DOE requirements, Table
30 2 summarizes the values of the present and the literature works in the field of hybrid CPCs filled
31 with carbon-based fillers. In most cases, mechanical strength, thermal conductivity, and/or
32 through-plane conductivity is not reported, which makes it difficult to have a complete
33 comparison. The mechanical strength, Young's modulus, and the thermal conductivity obtained in
34 the current work exceed the reported values for filler contents below 80wt%. Only one paper with
35 80wt% filler reports higher thermal conductivity of $16.4\text{W}\cdot\text{m}^{-1}\cdot\text{K}^{-1}$ [64]. The electrical conductivity
36 exceeds all the values reported for the CPCs with the same or lower content of hybrid fillers; but
37 it is lower than the values for CPCs with 80wt.% filler content, which is significantly higher than
38 63wt.% filler used here. Moreover, CPCs in this work were obtained by regular extrusion and
39 compression molding processes without any further modification to the materials or processes and
40 should be readily scalable. It is also noted that the processing temperature can still be further
41
42
43
44
45
46
47
48
49
50
51
52
53
54
55
56
57
58
59
60

increased (Figure 4) and since the strength significantly exceeds the requirement, the DAP content could also be further increased, which both facilitate the application of higher filler contents to further increase the electrical and thermal conductivity, if needed. In addition, due to the high thermal stability of PC, compared to the other polymers (PP and PE, Table 2), PC-based CPCs will be more suitable for high-temperature fuel cell applications. Therefore, PC-based composites enriched with hybrid carbon-based fillers and DAP plasticizer appear to be a promising alternative for current bipolar plate materials or any other application demanding high electrical and thermal conductivity.

Table 2: A comparison between the present work results and the literature of CPCs with hybrid carbon-based fillers toward BPP application.

Author	Year	Matrix	Total Filler (wt. %)	Electrical conductivity (S.cm ⁻¹)		Thermal Conductivity (W.m ⁻¹ .K ⁻¹)	Mechanical Properties (MPa)
				In-plane	Thru-plane		
Present work		PC	63	34.3	4.2	2.93	75.4 (Tensile strength) 3975 (Tensile modulus)
Naji et al. [35]	2017	PC	65	8.3	12.8	1.7	-
Krause et al. [64]	2017	PP	80	-	3.4	16.4	23.5 (Flexural strength) 5726 (Flexural modulus)
Bairan et al [31]	2016	PP	80	158	-	-	30 (Flexural)
Caglar et al. [65]	2014	PP	80	50	10	-	48.01 (Flexural)
Salemat et al [66]	2013	PP	80	296	-	-	-
Greenwood et al [67]	2012	PE	57	0.409	0.85	2.17	27 (Tensile strength) 37.7 (Flexural strength)
Yeetsorn [46]	2010	PP	55	13	1.2	0.31	30 (Flexural strength)
Mali [68]	2006	PP	54	12	2.2	-	27.7 (Tensile strength) 1697 (Tensile modulus) 82.8 (Flexural strength)
Wang [69]	2006	PP	65	19	1.56	-	9.5 (Tensile strength) 584 (Tensile modulus) 47.7 (Flexural strength)
US DOE Targets [5]	-	-	-	> 100	> 20	> 10	> 41 (Tensile strength) > 45 (Flexural strength)

5. CONCLUSION

In this work, polycarbonate-based CPCs filled with single filler (CNT), binary fillers (CNT-CF), and ternary fillers (CNT-CF-G) were fabricated using an extrusion process followed by compression molding. DAP was used as an effective plasticizer in the ternary CPCs to facilitate the processing at high filler loadings.

The microstructure, electrical conductivity (both through-plane and in-plane), thermal conductivity, and mechanical properties of the fabricated CPCs were systematically investigated by varying the filler contents. The SEM results indicated a good bonding between the CFs and the PC matrix as well as some interconnections between CF, G, and CNT fillers. In PC-CNT composites, both the electrical and thermal conductivities increased as a function of CNT content. The tensile strength, however, decreased as the CNT content was increased. In binary CPCs with a fixed 3wt.% CNT content, all the investigated properties were significantly enhanced as the CF content was increased from 0 to 30wt.%.

The processing difficulties of the ternary CPCs with a total filler loading of >53wt.% were successfully mitigated by the introduction of DAP as a plasticizer during melt extrusion. In addition to the significant reduction of the process temperature by 75°C, the introduction of 10.8wt.% DAP to PC-3wt.%CNT-20wt.%CF-30wt.%G composite enhanced its conductivity and strength. The best combination of the properties was obtained for the ternary CPC with a composition of PC-3wt.%CNT-30wt.%CF-30wt.%G-8wt.%DAP. The through-plane electrical, in-plane electrical, and thermal conductivities, area specific resistance, and tensile strength were 4.22S.cm⁻¹, 34.3S.cm⁻¹, 2.9W.m⁻¹.K⁻¹, 0.05Ω.cm², and 75.4MPa, respectively. These values were compared to the literature data and the DOE targets and it was concluded that PC-based composites

1
2
3 filled with hybrid fillers and plasticizer fabricated through simple extrusion process are potential
4
5 alternative materials for bipolar plate manufacturing.
6
7
8
9

10 11 **Acknowledgement**

12
13
14 The author express their gratitude to the following companies to provide us with the materials:
15
16 SABIC Company, Lyondell Basell Industries, Zoltek Corporation, Asbury Carbons Inc., and
17
18 Nanocyl S.A. The authors also thank the Ministry of Higher Education and Scientific Research of
19
20 Iraq for the financial support.
21
22
23

24 25 **References**

- 26
27 [1] E. Planes, L. Flandin, and N. Alberola, *Energy Procedia*, vol. 20, p. 311 – 323, 2012.
28 [2] X-Z. Yuan, H. Wang, J. Zhang, and D. P. Wilkinson, *Journal of new materials for electrochemical systems*,
29 vol. vol. 8, pp. 257-267, 2005.
30 [3] R. Taherian, *Journal of Power Sources*, vol. 265, pp. 370-390, 2014.
31 [4] P. Leung, X-H Li, C-P deon, L. Berlouis, CT J. Low, and P-C. Walsh, *RSC Adv*, pp. 10125-56, 2012.
32 [5] [Online]. Available: "www1.eere.energy.gov," [Online]. Available:
33 https://www1.eere.energy.gov/hydrogenandfuelcells/mypp/pdfs/fuel_cells.pdf.
34 [6] H. Tawfik, Y. Hung, and D. Mahajan, *Journal of Power Sources*, vol. 163, p. 755–767, 2007.
35 [7] S. Karimi, N. Fraser, B. Roberts, and F. R. Foulkes, *Advanced Materials Science and Engineering*, pp. 1-22,
36 2012.
37 [8] N. F. Asri, T. Husaini, A. Sulong, E. H. Majlan, and W. R. W. Daud, *International Journal of Hydrogen*
38 *Energy*, vol. 42, pp. 9135-48, 2017.
39 [9] S. A. Abo El-Enin, O. E. Abdel-Salam, H. El-Abd, and A. M. Amin, *Journal of Power Sources*, vol. 177, pp.
40 13-16, 2008.
41 [10] A. Heinzl, F. Mahlendorf, and C. Jansen, "Bipolar Plates," in *Fuel Cells – Proton-Exchange Membrane Fuel*
42 *Cells*, Duisburg, University of Duisburg–Esse, 2009, pp. 810-816.
43 [11] H. Suherman, A. Sulong and J. Sahari, *Ceramics International*, vol. 39, pp. 1277-1284, 2013.
44 [12] A. Ghosh, P. Goswami, P. Mahanta, and A. Verma, *J. Solid State Electrochem*, vol. 18, pp. 3427-3436, 2014.
45 [13] J. W. Lim, M. Kim, and D. G. Lee, *Composite Structures*, vol. 108, pp. 757-766, 2014.
46 [14] A. Adloo, M. Sadeghi, M. Masoomi, and H. N. Pazhooh, *Renewable Energy*, vol. 99, pp. 867-874, 2016.
47 [15] A. Ameli, M. Nofar, S. Wang, and C. B. Park, *ACS applied materials & interfaces*, vol. 6, no. 14, pp. 11010-
48 11019, 2014.
49 [16] Y. Kazemi, A.R. Kakroodi, A. Ameli, T. Filleter, and C.B. Park, *RSC Journal of Materials Chemistry C*, vol.
50 6, pp. 350-359, 2018.
51
52
53
54
55
56
57
58
59
60

- 1
2
3 [17] Y. Kazemi, A.R. Kakroodi, S. Wang, A. Ameli, T. Filleter, P. Pötschke, and C.B. Park, *Polymer* (United
4 Kingdom) vol. 129, pp. 179-188, 2017.
5
6 [18] A. Ameli, S. Wang, Y. Kazemi, C. B. Park, and P. Pötschke, *Nano Energy*, vol. 15, pp. 54-65, 2015.
7 [19] A. Ameli, M. Arjmand, P. Pötschke, B. Krause, and U. Sundararaj, *Carbon*, vol. 106, pp. 260-278, 2016.
8 [20] M. Arjmand, A. Ameli, and U.-T. Sundararaj, *Macromolecular Materials and Engineering*, vol. 301, pp. 555-
9 565, 2016.
10
11 [21] S. Sathyanarayana and C. Hübner, *Thermoplastic Nanocomposites with Carbon Nanotubes in Structural*
12 *Nanocomposites, Perspectives for Future Applications*, Verlag Berlin Heidelberg: Springer, 2014.
13 [22] B. D. Cunningham, J. Huang, and D. G. Baird, *Journal of Power Sources*, vol. 165, pp. 764-773, 2007.
14 [23] C. Hopmann, C. Windeck, A. Cohnen, J. Onken, B. Krause, P. Pötschke, and T. Hickmann, *AIP Conference*
15 *Proceedings 1779*, 2016.
16 [24] P. Rzeczkowski, M. Lucia, A. Müller, M. Facklam, A. Cohnen, P. Schäfer, C. Hopmann, T. Hickmann, P.
17 Pötschke and B. Krause, *AIP Conference Proceedings*, Accepted.
18 [25] B. Krause, P. Pötschke and T. Hickmann, *AIP Conference Proceedings*, Accepted.
19 [26] P. Greenwood, R. Chen and R. H. Thring, *Journal of Materials: Design and Applications*, vol. 222, pp. 197-
20 208, 2008.
21 [27] L. Xia, A. Li, W. Wang, Q. Yin, H. Lin, and Y. Zhao, *Journal of Power Sources*, vol. 178, pp. 363-367, 2008.
22 [28] T. Yang and P. Shi, *Journal of Power Sources*, vol. 175, pp. 390-396, 2008.
23 [29] R. B. Mathur, S. R. Dhakate, D. K. Gupta, T. L. Dhami and R. K. Aggarwal, *Journal of Materials Processing*
24 *Technology*, vol. 203, pp. 184-192, 2008.
25 [30] S. Liao, C. Yen, C. Weng, Y. Lin, C. M. Ma, C. Yang, M. Tsai, M. Yen, M. Hsiao, S. Lee, X. Xie and Y.
26 Hsiao, *Journal of Power Sources*, vol. 185, pp. 1225-1232, 2008.
27 [31] A. Bairan, M. Selamat, S. N. Sahadan, S. D. Malingam and N. Mohamad, *Procedia Chemistry*, vol. 19, pp.
28 91-97, 2016.
29 [32] R. Yeetsorn, M. W. Fowler and C. Tzoganakis, "A Review of Thermoplastic Composites for Bipolar Plate
30 Materials in PEM Fuel Cells," in *Nanocomposites with Unique Properties and Applications in Medicine and*
31 *Industry*, Croatia, Slavka Krautzeka 83/A 51000 Rijeka, 2011, p. 360.
32 [33] M. Kim, J. W. Lim, K. H. Kim and D. G. Lee, *Composite Structures*, vol. 96, pp. 569-75, 2013.
33 [34] A. Iwan, M. Malinoski and G. Pasciak, *Renewable and Sustainable Energy Reviews*, vol. 49, pp. 954-967,
34 2015.
35 [35] A. Naji, B. Krause, P. Pötschke, and A. Ameli, *Polymer Composites*, 2018, in press, doi: 10.1002/pc.25169.
36 [36] A. Ameli, Y. Kazemi, S. Wang, C.B. Park and P. Pötschke, *Composites: Part A*, vol. 96, pp. 28-36, 2017.
37 [37] M. Grundler, T. Derieth, and A. Heinzl, "Polymer compounds with high thermal conductivity," in *AIP*
38 *Conference Proceedings 1779*, 030015, 2016.
39 [38] T. Derieth, G. Bandlamudi, P. Beckhaus, C. Kreuz, F. Mahlendorf, and A. Heinze, *Journal of New Materials*
40 *for Electrochemical Systems*, vol. 11, pp. 21-29, 2008.
41 [39] B. Krause, A. Cohnen, P. Pötschke, T. Hickmann, D. Koppler, B. Proksch, T. Kersting, and Ch. Hopmann,
42 *AIP Conference Proceedings 1914*, 030009, 2017.
43 [40] J. Zhou and G. Lubineau, *ACS Applied Materials and Interfaces*, vol. 5, pp. 6189-6200, 2013.
44 [41] J. Zhou, I. A. Ventura and G. Lubineau, *Industrial and Engineering Chemistry Research*, vol. 53, pp. 3539-
45 3549, 2014.
46 [42] A. Patole, I. Aguilar Ventura and G. Lubineau, *Journal of Applied Polymer Science*, vol. 132, pp. 422-81,
47 2015.
48
49
50
51
52
53
54
55
56
57
58
59
60

- 1
2
3 [43] A. Király and F. Ronkay, *Polymers & Polymer Composites*, vol. 21, no. 2, pp. 93-100, 2013.
- 4 [44] B. Krause and P. Pötschke, *AIP Conference Proceedings 1779*, 040003, 2016.
- 5 [45] B. A. Johnson, Thermally and Electrically Conductive Polypropylene Based Resins for Fuel Cell Bipolar
6 Plates, Michigan State: Chemical Engineering, Michigan Technological University, 2009.
- 7 [46] R. Yeetsorn, Development of Electrically Conductive Thermoplastic Composites for Bipolar Plate Application
8 in Polymer Electrolyte Membrane Fuel Cell, *doctorate thesis*, Ed., Ontario: Waterloo University, 2010.
- 9 [47] Nanocyl, Data sheet Nanocyl 7000, 2007-02-05 ed., Sambreville, 2007.
- 10 [48] B. Krause, R. Boldt, and P. Pötschke, "method for determination of length distributions of multiwalled carbon
11 nanotubes before and after melt processing," *Carbon*, vol. 49, pp. 1243-1247, 2011.
- 12 [49] N. Afiqah, M. Radzuan, M. Y. Zakaria and A. Sulong, *Composites Part B*, vol. 110, pp. 153-160, 2017.
- 13 [50] H. E. Lee, Y. S. Chung and S. S. Kim, *Composite Structures*, vol. 180, pp. 378-385, 2017.
- 14 [51] H. E. Lee, S. H. Han, S. A. Song and S. S. Kim, *Composite Structures*, vol. 134, pp. 44-51, 2015.
- 15 [52] J. W. Kim, N. H. Kim, T. Kuilla, T. J. Kim, K. Y. Rhee and J. H. Lee, *Journal of Power Sources*, vol. 195, pp.
16 5474-5480, 2010.
- 17 [53] M. M. Larijani, E. J. Khamse, J. Davoodi, F. Ziaie, S. Safa, K. Arbabi and M. A. Taghavizadeh,
18 *Optoelectronics and Advanced Materials*, vol. 5, pp. 252-257, 2011.
- 19 [54] S. Nam, D. Lee, D. G. Lee and J. Kim, *Composite Structures*, vol. 159, pp. 220-227, 2017.
- 20 [55] J. O. Alhamid, C. Mo, X. Zhang, P. Wang, M. D. Whiting, and Q. Zhang, *Biosystems Engineering*, vol. 172,
21 pp. 124-33, 2018.
- 22 [56] B. Krause, T. Villmow, R. Boldt, M. Mende, G. Petzold and P. Pötschke, *Composites Science and
23 Technology*, vol. 71, pp. 1145-1153, 2011.
- 24 [57] X. Tian, M. E. Itkis, E. B. Bekyarova, and R. C. Haddon, *Scientific Reports*, vol. 3, pp. 1-6, 2013.
- 25 [58] Genhai G. Liang, W. D. Cook, H. J. Sautereau and A. Tcharkhtchi, *European Polymer Journal*, vol. 44, pp.
26 366-75, 2008.
- 27 [59] R. A. Antunes, M. C.L. d. Oliveira, G.d Ett and V. Ett, *Journal of Power Sources*, vol. 196, pp. 2945-2961,
28 2011.
- 29 [60] P. Pötschke, A. R. Bhattacharyya, A. Janke, S. Pegel, A. Leonhardt and C. Täschner, *Journal of Fullerenes,
30 Nanotubes and Carbon Nanostructures*, vol. 13, pp. 211-224, 2005.
- 31 [61] B. Hornbostel, P. Pötschke, J. Kotz and S. Roth, *Physica E: Low-dimensional Systems and Nanostructures*, vol.
32 40, pp. 2434-2439, 2008.
- 33 [62] F. Y. Castillo, R. Socher, B. Krause, R. Headrick, B. P. Grady, R. Prada-Silvy and P. Pötschke, *Polymer*, vol.
34 52, pp. 3835-3845, 2011.
- 35 [63] K. H. Kim and W. H. Jo, *Carbon*, vol. 47, pp. 1126-1134, 2009.
- 36 [64] B. Krause, A. Cohnen, P. Pötschke, T. Hickmann, D. Koppler, B. Proksch, T. Kersting, and Ch. Hopmann,
37 *AIP Conference Proceedings 1914*, 030009, 2017.
- 38 [65] B. Caglar, J. Richards, P. Fischer and J. Tuebk, *Advanced Materials Letters*, vol. 5, pp. 299-308, 2014.
- 39 [66] M. Z. Selamat, M. S. Ahmad, M. A. D. Mohd amd N. Ahmad, *Advanced Materials Research*, vol. 795, pp. 29-
40 34, 2013.
- 41 [67] P. Greenwood, R. Thring and R. Chen, *J Materials: Design and Applications*, vol. 3, pp. 226-242, 2012.
- 42 [68] T. J. Mali, Thermoplastic composites for polymer electrolyte membrane fuel cell bipolar plates, Ontario:
43 Waterloo, 2006.
- 44
45
46
47
48
49
50
51
52
53
54
55
56
57
58
59
60

1
2
3
4
5
6
7
8
9
10
11
12
13
14
15
16
17
18
19
20
21
22
23
24
25
26
27
28
29
30
31
32
33
34
35
36
37
38
39
40
41
42
43
44
45
46
47
48
49
50
51
52
53
54
55
56
57
58
59
60

[69] Y. Wang, Conductive thermoplastic composite blends for flow field plates for use in polymer electrolyte membrane fuel cells (PEMFC), M. Thesis, Ed., Ontario: Waterloo University, 2006.